Adv. Radio Sci., 9, 9–17, 2011
www.adv-radio-sci.net/9/9/2011/
doi:10.5194/ars-9-9-2011

Advances in Radio Science

Verification of scattering parameter measurements in waveguides up to 325 GHz including highly-reflective devices

T. Schrader[1], **K. Kuhlmann**[1], **R. Dickhoff**[1], **J. Dittmer**[1], **and M. Hiebel**[2]

[1]Physikalisch-Technische Bundesanstalt, Braunschweig, Germany
[2]Rohde & Schwarz, Munich, Germany

Abstract. Radio-frequency (RF) scattering parameters (S-parameters) play an important role to characterise RF signal transmission and reflection of active and passive devices such as transmission lines, components, and small-signal amplifiers. Vector network analysers (VNAs) are employed as instrumentation for such measurements. During the last years, the upper frequency limit of this instrumentation has been extended up to several hundreds of GHz for waveguide measurements. Calibration and verification procedures are obligatory prior to the VNA measurement to achieve accurate results and/or to obtain traceability to the International System of Units (SI). Usually, verification is performed by measuring well-matched devices with known S-parameters such as attenuators or short precision waveguide sections (shims). In waveguides, especially above 110 GHz, such devices may not exist and/or are not traceably calibrated. In some cases, e.g. filter networks, the devices under test (DUT) are partly highly reflective. This paper describes the dependency of the S-parameters a) on the calibration procedure, b) on the applied torque to the flange screws during the mating process of the single waveguide elements. It describes further c) how highly-reflective devices (HRD) can be used to verify a calibrated VNA, and d) how a measured attenuation at several hundreds of GHz can be substituted by a well-known coaxial attenuation at 279 MHz, the intermediate frequency (IF) of the VNA, to verify the linearity. This work is a contribution towards traceability and to obtain knowledge about the measurement uncertainty of VNA instrumentation in the millimetre-wave range.

1 Introduction

With the development of millimetre-wave instrumentation e.g. VNA mainframes and waveguide frequency extensions (Fig. 1), more and more insight is gained in network analysis at frequencies beyond 110 GHz (Adamson et al., 2009). In general, network analysis is a necessary tool for development and testing, also at millimeter-wave frequencies. Many applications benefit from the development of this versatile instrumentation. Some practical examples are the characterisation of passive and active devices, calibration of antennas, systems, and material properties. The waveguide VNA technology is applied e.g. to characterise signal propagation to develop future ultrafast and high-bitrate data transfer systems and communication links (Jastrow et al., 2010; Priebe et al., 2010), to characterise absorber material or anechoic environments using time-domain techniques (Schrader et al., 2010) or to measure the response of field probes at millimetre wavelengths (Salhi et al., 2010).

Before usage, any VNA has to be calibrated with respect to the measurement ports at the reference plane. Typical calibration procedures such as TMSO, TRL, and LRL are applicable also in the waveguide system (T: through, M: match, S: short, O: open – here offset short, L: line, R: reflect).

With increasing frequency it becomes more difficult to design a well-matched load or an open standard. Hence, TRL, LRL, and offset-short calibrations become more important at higher frequencies. Furthermore, with increasing frequency losses due to the skin effect become more significant. Moreover, surface roughness becomes a major factor with respect to losses and wave propagation (Hoffmann, 2009). In general, mechanical dimensions and their deviations from the ideal geometry become more critical. Therefore, high precision manufacturing of waveguides and components becomes a crucial factor with respect to the measurement uncertainty.

Correspondence to: T. Schrader
(thorsten.schrader@ptb.de)

Published by Copernicus Publications on behalf of the URSI Landesausschuss in der Bundesrepublik Deutschland e.V.

Fig. 1. VNA mainframe and sets of frequency converters covering the WR15, WR10, WR6, WR5, and WR3 waveguide bands.

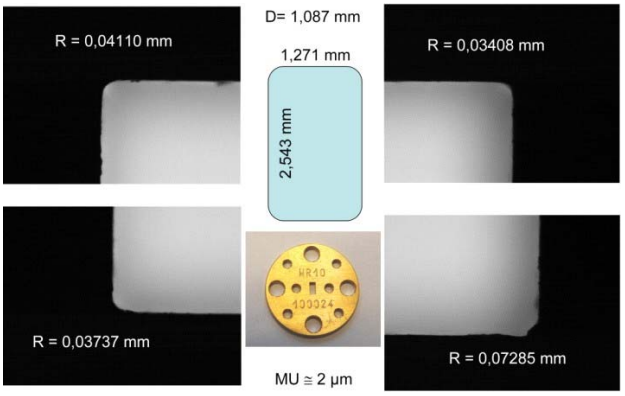

Fig. 2. Zoom images of the edges of the WR10 waveguide shim. The radii R and the waveguide square dimensions, the thickness of the shim, and the measurement uncertainty MU are given.

During calibration, several standards are connected to each VNA measurement test port. In addition, a through and – depending on the used calibration method – a waveguide of short length (shim) or shims with different line lengths are inserted between the measurement ports. Mating of the flanges is supported by four alignment pins, and for precision flanges by two additional dowel pins. By this the remaining uncertainty due to the waveguide mating process is reduced to a minimum but still leads to irregularities along the line (Stumper, 2001; Lau, 2010; Lok et al., 2009), again increasing with frequency. After mating of the flanges the connection is fixed by four screws around the flange. Only precision flanges have an additional "anti-cocking" rim to avoid air gaps between the mating planes or mechanical misalignment due to non-uniform screw torque. As waveguide flanges may be manufactured from thin or weak materials, the applied screw torque should be well-defined using a torque wrench. This tool also ensures a flange mating with a repeatable force both at calibration and measurements.

Typically, after calibration a known device is measured as verification standard (Clarke et al., 2009; Ridler et al., 2010a, 2010b; Horibe et al., 2010). Its properties may be known from prior and other calibration measurements, mechanical measurements, analytical calculations, or other methods of characterisation. Precision gold-plated shims provide a quarter-wavelength transmission phase shift at the band mid frequency. The input reflection coefficient of the shim as thru device is dominated by a) the waveguide cross-sectional mechanical dimensions and b) by the effective load match of the output port (Williams, 2010), (Judaschke, 2011). If the thru device is highly reflective instead of being a perfect waveguide also the effective source match generates an input standing wave. Furthermore, the effective directivity at both test ports has significant influence on the measurement result. Both effects of effective source and load match and effective directivity play an important role determining the S-parameters of DUTs, especially for highly reflective devices (HRD), which belong to the most challenging type of DUTs. Such a HRD could be e.g. a filter network offside its pass-band. A well-matched attenuator as a typical verification device does not reveal the effects of effective directivity and/or effective source and load match. Usually, a precision waveguide section, a short and a match are used to apply the classical ripple method, thus identifying the effective directivity and source and load match. The methods described here are an alternative to the classical ripple method as precision waveguide sections are not available yet.

Measurements of filter networks typically require a high dynamic range of the instrumentation. As VNAs offer a high dynamic range, linearity has to be guaranteed for precise high attenuation measurements and therefore to be verified experimentally. To investigate the VNA linearity, we compare a known RF attenuation inserted between the test ports with a calibrated coaxial attenuator (at 279.28 MHz) inserted in the "meas input" path of the VNA.

2 The equipment

2.1 Instrumentation

We have used a 4-port vector network analyser R&S ZVA 50 GHz with frequency converters (type ZVA-Z, cp. Fig. 1) covering the frequency range of the corresponding waveguide bands 50–75 GHz (WR15), 75–110 GHz (WR10), 110–170 GHz (WR6), 140–220 GHz (WR5), and 220–325 GHz (WR3). The waveguide calibration kits (R&S ZV-WR) are corresponding to the waveguide bands above. We have used the kits with fixed loads. An adjustable WR10 precision rotary attenuator (0–60 dB, Flann 27110) and PC3.5 mm coaxial precision fixed attenuators (Rosenberger 03AS102, with 3 dB, 6 dB, 10 dB, 20 dB, and three 30 dB attenuators) were

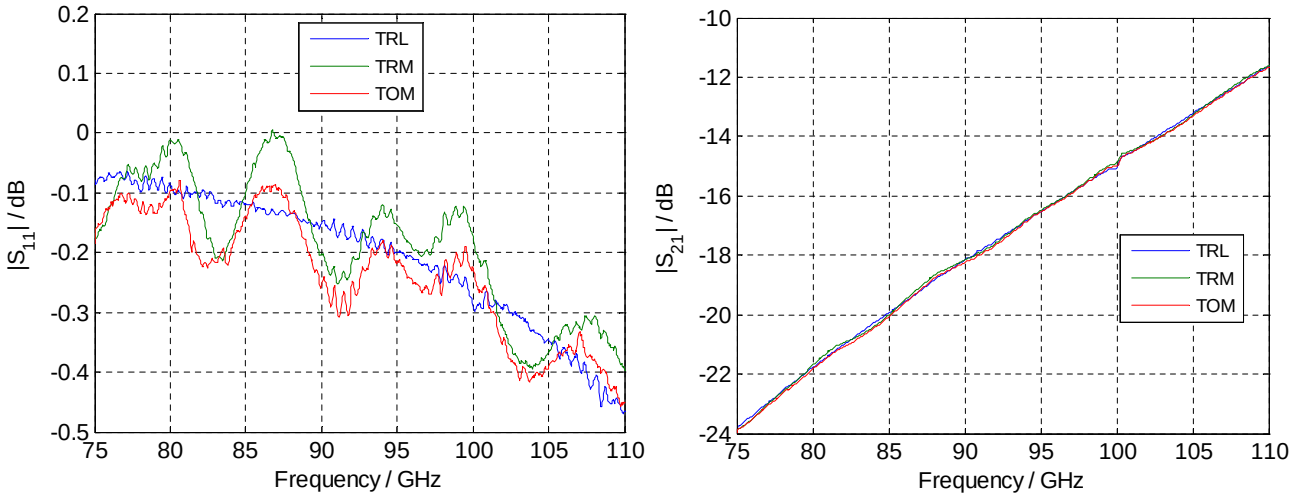

Fig. 3. Measured S-parameters of the HRD type "90° shim" for different calibrations schemes.

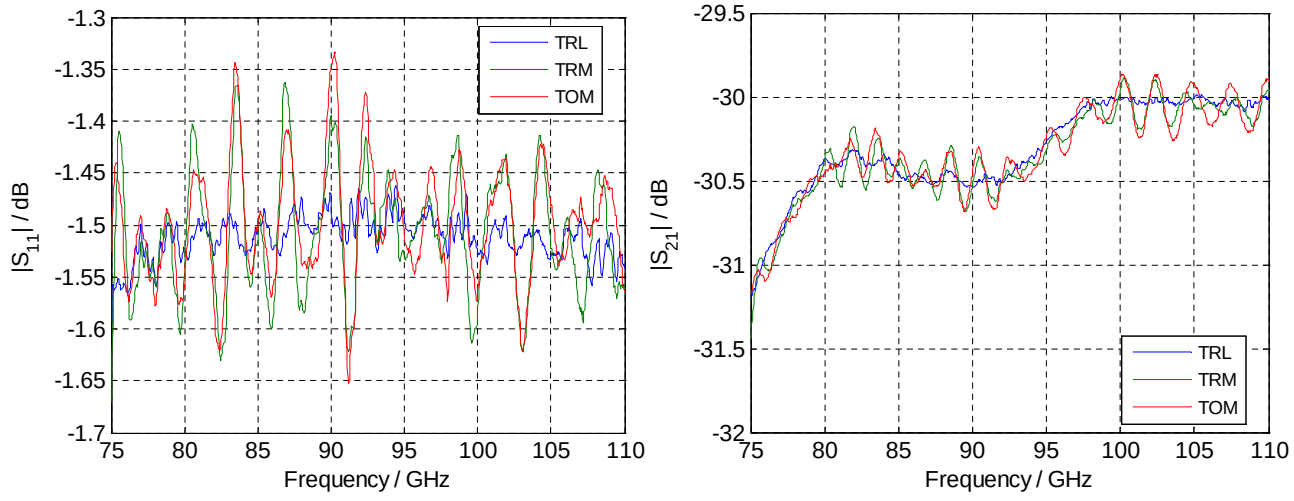

Fig. 4. Measured S-parameters of the HRD type "thin foil" obtained by applying different calibration schemes.

used for the linearity measurements. The higher values 40 dB, 50 dB, and 60 dB were assembled from (10 + 30) dB, (20 + 30) dB and (30 + 30) dB attenuators.

2.2 Design and characterisation of highly reflective devices (HRD)

We have used three different kinds of HRDs. First, a 125 µm polyimide foil (Goodfellow) coated with a thin one-sided thermal deposition Titanium layer of about 60 nm was assembled between the test port waveguide flanges. Therefore, ohmic contact to the flanges is only possible at one side. The Titanium layer is very stable with respect to the mechanical stability and oxidation. As the thickness of the metal layer is kept 10 times below the smallest skin depth of about 550 nm, the resulting attenuation does not change with frequency. We obtained a nearly constant frequency response in all used waveguide bands (cp. Sect. 2.1) from 50 GHz up to 325 GHz.

The second HRD was a regular shim as part of the waveguide calibration kit, that was rotated by 90 degrees before mounting. Thereby the shim changes its behaviour from a matched line section to a waveguide below cut-off. The evanescent mode in the rotated shim provides a low transmission. The attenuation only depends on the mechanical dimensions while surface roughness and skin effect losses can be neglected due to the short line length. Mechanical measurements on an optical coordinate measuring machine provided the exact shim dimensions, as shown in Fig. 2 for the WR10 shim. Here, the pixel resolution of the optical image was about one µm, the measurement uncertainty was 2 µm. The thickness D of the shim was determined to be

Table 1. Contributions to the measurement uncertainty of reflection and transmission (in dB) for a HRD and a temperature range of 22.7 °C to 24.2 °C.

	torque		Drift 17 h		model simulation		calibration		attenuation	repro-ducibility	
in dB	$\lvert S_{ii}\rvert$	$\lvert S_{ij}\rvert$	$\lvert S_{ii}\rvert$	$\lvert S_{ij}\rvert$	$\lvert S_{ii}\rvert$	$\lvert S_{ij}\rvert$	$\lvert S_{ii}\rvert$	$\lvert S_{ij}\rvert$	$\lvert S_{ij}\rvert$	$\lvert S_{ii}\rvert$	$\lvert S_{ij}\rvert$
WR15	0.1	0.05	0.01	0.02	0.1	0.1	n.a.		n.a.	0.03	0.05
WR10	0.1	0.1	0.02	0.05	0.1	0.1	0.15	0.25	0.1	0.05	0.05
WR6	0.25	0.2	0.05	0.05	0.1	0.1	n.a.		n.a.	0.05	0.05
WR5	0.25	0.2	0.05	0.05	0.15	0.5	n.a.		n.a.	0.05	0.05
WR3	1.0	0.25	0.1	0.3	0.5	0.5	1.0	1.0	n.a.	0.1	0.5

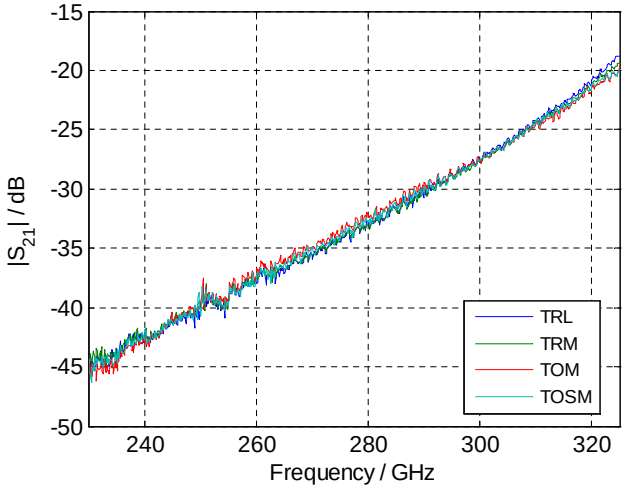

Fig. 5. Measured S-parameters of the HRD type "shim with cylindrical hole" obtained by applying different calibration schemes.

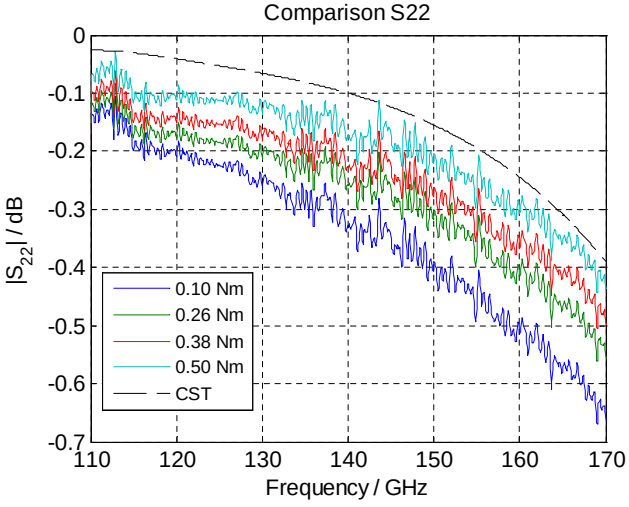

Fig. 6. Measurement of S_{22} of the HRD type "90° shim" in WR6 waveguide using a torque wrench compared with CST simulations. The waveguide connection was opened and completely re-assembled for each torque setting.

1.087 mm, the waveguide cross-sectional dimensions were 2.543 mm × 1.271 mm.

Again, this HRD type was used in all waveguide bands (cp. Sect. 2.1).

The third HRD was a shim of 1 mm thickness made of brass with a cylindrical hole of 500 µm diameter manufactured with a precision reamer. Here, we have used this HRD only in the WR3 waveguide band, by choosing the diameter accordingly, it can be used for the lower bands as well.

The numerical computations were performed using CST Microwave Studio (Computer Simulation Technology, www.cst.com, Darmstadt, Germany). To model the thin metal foil a conductive non-metallic material has to be chosen instead of a lossy metal. In a second step, the material was assigned the conductivity of Ti ($\sigma = 2.56 \cdot 10^6$ S/m).

2.3 Assembly

In order to determine the dependency of the scattering parameters S_{ii} and S_{ij} on the mechanical torque applied to the mounting screws at the waveguide flanges we used straight and 90° offset torque wrenches.

3 Measurement results

For VNA calibration we used the standard firmware procedures. The measurements were performed in a laboratory environment without air-conditioning. The temperature was monitored in the range between 22.7 °C and 24.2 °C. We also measured the hardware drift during 17 h. All VNA measurements were performed with 801 frequency points and a resolution bandwidth of 100 Hz. We applied 5 averages per frequency point.

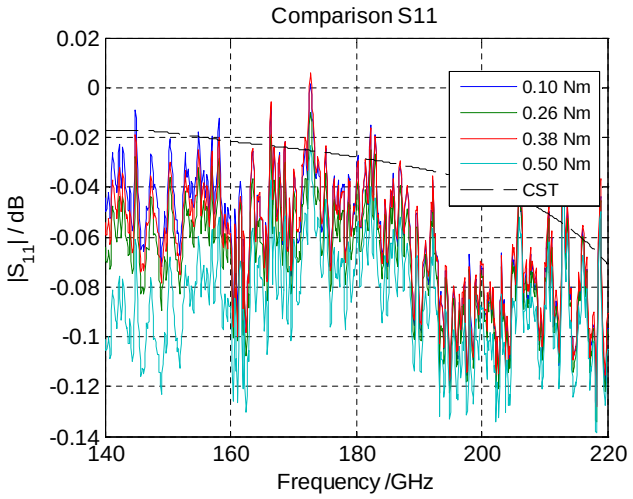

Fig. 7. Measured and simulated magnitude of S_{11} of the HRD type "90° shim" in WR5 waveguide using a torque wrench.

3.1 Dependency of scattering parameters on the calibration scheme

To investigate the influence of the calibration method on the measured S-parameters, we have performed different calibrations. Subsequently measurements of the HRD (90° shim) have been performed, as can be seen in Fig. 3. The abbreviations of the calibration standards are T: through, R: reflect (short), L: line (shim in regular orientation), M: broadband match, O: offset short (built from shim and short of the calibration kit).

Secondly, we used the HRD type "thin foil" as DUT. The results are shown in Fig. 4. Obviously, the deviations of S-parameters due to different calibration schemes depend on the DUT (and its length). For the HRD type "90° shim", S_{11} varies slowly with frequency, but for the HRD type "thin foil" S_{11} changes much faster with frequency, but with almost similar amplitude. The TRL scheme shows the best performance as the frequency response is rather flat compared to TRM and TOM. The variations of $|S_{21}|$ in Figs. 3 and 4 show the same behaviour and frequency response. For the WR3 waveguide and HRD type "shim with cylindrical hole" we obtained a continuously increasing frequency response with superimposed oscillations in the order of 1 dB, depicted in Fig. 5.

All results of the dependency of S-parameters on the calibration scheme are summarised in Table 1.

3.2 Influence of the fastening torque on S-Parameters

A parametric study was performed in order to identify the influence of the fastening torque of the flange screws to assemble the waveguide devices. The torque was increased from 0.1 nm to 0.5 nm in steps of 0.04 nm using the same torque wrench (cp. Figs. 6–8).

It can be noted that the S-parameters are significantly depending on the applied torque. The reflection parameters S_{ii} values show a much higher sensitivity on the torque than the transmission parameters S_{ij}. Increasing the torque from 0.1 nm to 0.5 nm brings S_{22} closer to the theoretical reflection. The increasing torque reduces the ohmic contact resistance between waveguide and shim by reducing the remaining gaps between the flanges. As the axes of DUTs and test ports are not perfectly in line, these investigations are only possible, if the frequency converters are not fixed on the workbench.

It is evident in Figs. 6 and 8, that for the WR6 and WR3 waveguides increasing the torque matches simulation and measurement better, whereas in Fig. 7 the reproducibility limit for the WR5 waveguide is reached. The initial alignment of the WR5 waveguide was better than that of WR6. For a precision measurement it is crucial, that mating of the flanges is done without mechanical stress due to axial misalignment. The reproducibility of flange mating was tested by assembling, opening and re-assembling one waveguide connection ten times using 0.3 nm for all waveguide bands. The results are given in Table 1. It can be seen, that reproducibility and hardware drift are not the major contributions to uncertainty. The influence of the measurement bandwidth on the S-parameters was not tested yet.

3.3 Measurement and simulation of S-parameters of highly reflective devices (waveguide shims)

Usually, well-matched attenuators are used for verification of calibrated VNAs. However, in the millimetre-wave range, especially beyond 110 GHz, a traceable calibration of such devices is not available yet. To make progress in that regard, we have used regular waveguide shims according to Sect. 2.2 for that purpose. They are mechanically stable devices and can be characterised by their mechanical dimensions. Instead of mounting them correctly we have rotated them by 90° and inserted them as iris into the waveguide setup. Due to the increasing coupling with frequency, the response of S_{21} covers about 10 dB dynamic range within the WR10 waveguide band as shown in Fig. 9 and about 23 dB in the WR6 waveguide band, respectively. The resulting differences between simulation and measurement are listed in Table 1. It can be seen that numerical simulations predict the measurement results quite closely, especially for the HRD 90°.

3.4 Verification of linearity by substituting the RF attenuation by an IF attenuation

3.4.1 DUT A: precision WR10 rotary attenuator

In order to compare a known RF attenuation with traceably calibrated coaxial attenuators in the MHz range we used a precision WR10 rotary attenuator (PRA) having a maximum attenuation of 60 dB. As the frequency response of the PRA

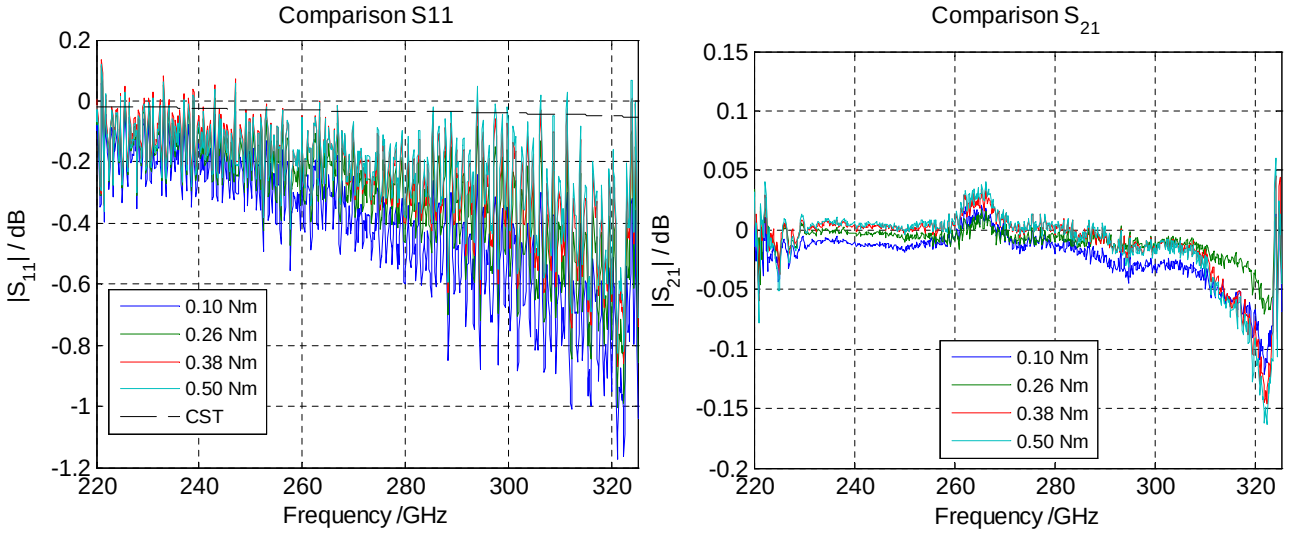

Fig. 8. Comparison of measured S-parameters of the HRD type "90° shim" using shim #2 (the WR3 calibration kit contains two shims with different length) and of the through connection using a torque wrench. The connection between the WR3 waveguides was opened and completely re-assembled for each torque setting.

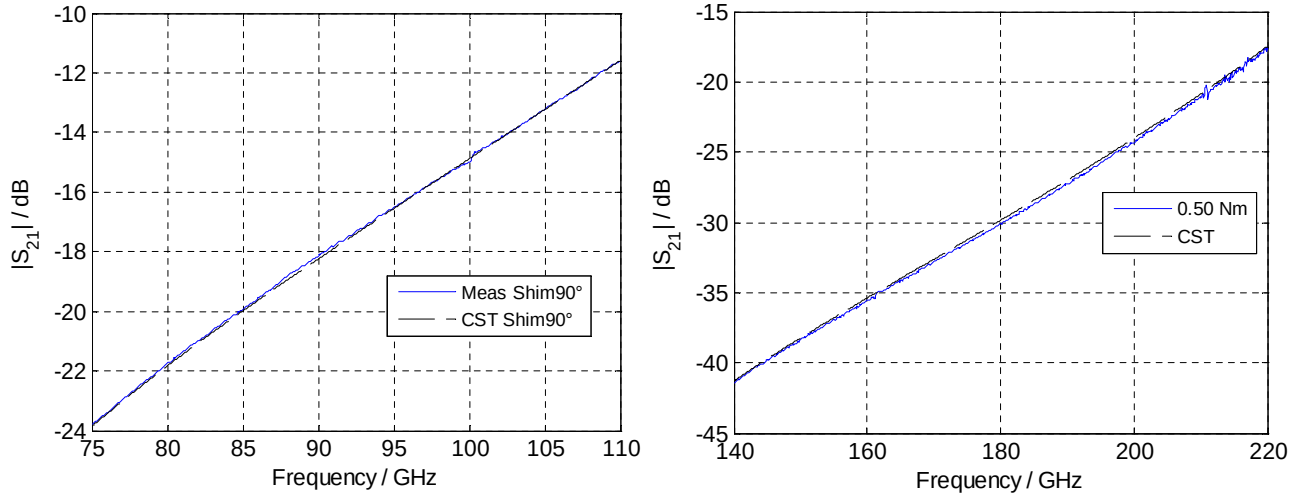

Fig. 9. Numerical simulation (CST) and measurement of S_{21} of a WR10 and a WR6 shim each rotated by 90°.

is nearly independent of frequency and the attenuation setting, we can compare a presumably known RF attenuation inserted between the test ports with a coaxial attenuator which is precisely calibrated at 279.28 MHz (the IF of the VNA) and inserted in the "meas input" path of the VNA (Fig. 10). Under the assumption that input and output reflection coefficient of the hardware of the "meas input" path of the VNA are low, inserting the coaxial attenuators does not substantially raise the mismatch uncertainty in the "meas in" path. The traceably calibrated attenuation values of the coaxial attenuators can therefore be used for comparison. We have chosen combinations of such coaxial attenuators to cover the dynamic range. Furthermore, we have assumed that the small reflection coefficients at the in- and output ports of the attenuators do not show a significant influence on the total attenuation due to the VSWR when mounting the attenuators in series.

The regular signal at 279.28 MHz as sent from the frequency converter to the "meas in" port is a measure for the attenuation A_{GHz} of the attenuator in the GHz range inserted between the test ports, leading to an indication of $|S_{21\mathrm{GHz}}|$. Then, the attenuator is replaced by a thru. Subsequently, we insert a well-known attenuation (A_{MHz}) into the "meas in" path and read the indication $|S_{21,\mathrm{MHz}}|$. Ideally,

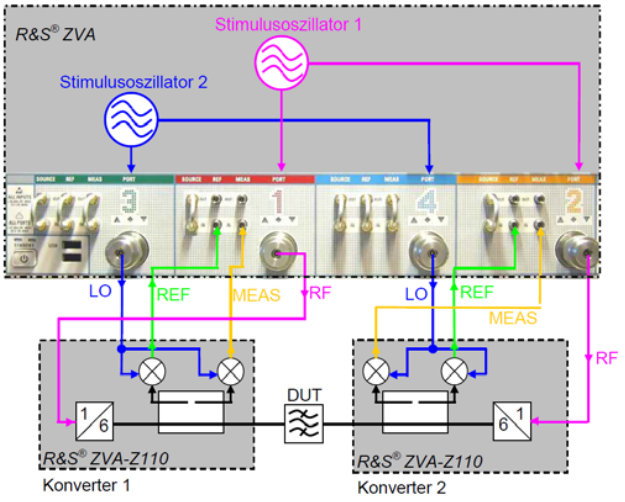

Fig. 10. Setup of VNA mainframe and frequency converters. The coaxial attenuator is inserted into the "Meas" connection at port 2.

$D_S = |S_{21,\mathrm{GHz}}| - |S_{21,\mathrm{MHz}}| = 0$. If A_{GHz} and A_{MHz} were *both* traceable quantities, D_S would indicate the deviation from linearity of the instrumentation (VNA hardware). Here, we only assume an attenuation A_{GHz} of the PRA, but we have used a traceably defined A_{MHz}.

We applied the following procedure: We have measured the frequency response for a 0 dB setting of the PRA and observed a typical flat frequency response with a dip at 88 GHz (see Fig. 11) and a low floor attenuation, even for a 0 dB setting. The frequency response did not change regardless of the attenuation setting (cp. Fig. 11). The floor residual attenuation was measured at 100 GHz each time the PRA was set to 0 dB. From 10 measurements we obtained 1.25 ± 0.02 dB. We have then taken the attenuation value from the calibration certificate, e.g. 9.918 dB for the nominal 10 dB attenuator, and adjusted the PRA to the calibrated value of the attenuator (in this example 9.9 dB). We took the marker value at 100 GHz again which was now -11.15 dB. After we have taken the S-parameter measurements, we set the PRA back to zero attenuation and inserted the attenuator into the coaxial "meas in" branch of the VNA. We took again the S-parameter measurements and the marker value at 100 GHz which was -11.17 dB. The differences of the marker readings with either the PRA or the coaxial attenuator in place were in the order of 0.01 dB up to 0.05 dB. These results show on the one hand that the setting of the PRA (indication to actual value) is very accurate (but not traceable by itself) and on the other hand that the linearity of the frequency converter is excellent (Fig. 11).

3.4.2 DUT B: highly reflective device (90° shim)

As a second device for linearity verification we have used the HRD 90° shim. Again, we have chosen combinations of the coaxial attenuators to cover the dynamic range. The theoretical value of the A_{GHz} attenuation of the 90° shim is obtained from numerical simulations using CST (cp. Sect. 2.2). Its mechanical data were traceably measured (cp. Sect. 2.2). The black circles in Fig. 12 indicate the intercept points of the GHz attenuation of the HRD 90° shim and the A_{MHz} attenuation in the "meas in" path overlap. Table 1 indicates a maximum deviation of S_{21} between simulation and measurement of 0.1 dB for WR10. As shims are part of standard calibration kits they are standard equipment. In combination with traceably calibrated coaxial attenuators they provide a convenient method for VNA verification up to the highest frequencies of interest.

4 Conclusions

Verification of vector network analysers in the millimetre- and sub-millimeter wave range can not yet make use of traceably calibrated attenuators at these high frequencies due to the lack of calibration facilities. Often, devices under test (DUT) exhibit a purely reflective behaviour, then a prior verification of the VNA using only low-reflective calibrated attenuators would not reveal effects such as effective load and source match errors or effective directivity, but the measured S-parameters of the DUT would induce these effects.

Therefore, we have introduced three different types of highly reflective devices (HRD) being suitable for verification in the millimetre- and submillimeter-wave bands including their mechanical and computational characterisation. We have shown that measurements of S-parameters of these HRD can depend strongly on the calibration procedure. Assembling of waveguides should only be done using torque wrenches as the S-parameters depend on the mating forces of the flanges.

Furthermore we have shown that a known millimetre-wave attenuation e.g. from a 90° rotated waveguide shim can be substituted by a traceably and precisely calibrated coaxial PC3.5 mm attenuator being inserted in the measurement path between the frequency converter and the VNA.

Acknowledgements. The authors thank their colleagues at PTB, Dr. Ulrich Neuschäfer-Rube and Dieter Schulz ("Multisensor Coordinate Metrology Group") for the mechanical measurements, Dirk Schubert ("High-frequency Measuring Techniques Group") for the precision RF calibration of the attenuators, and Daniel Hagedorn ("Surface Technology Group") for coating polyimide foils with thermal deposition of Titanium.

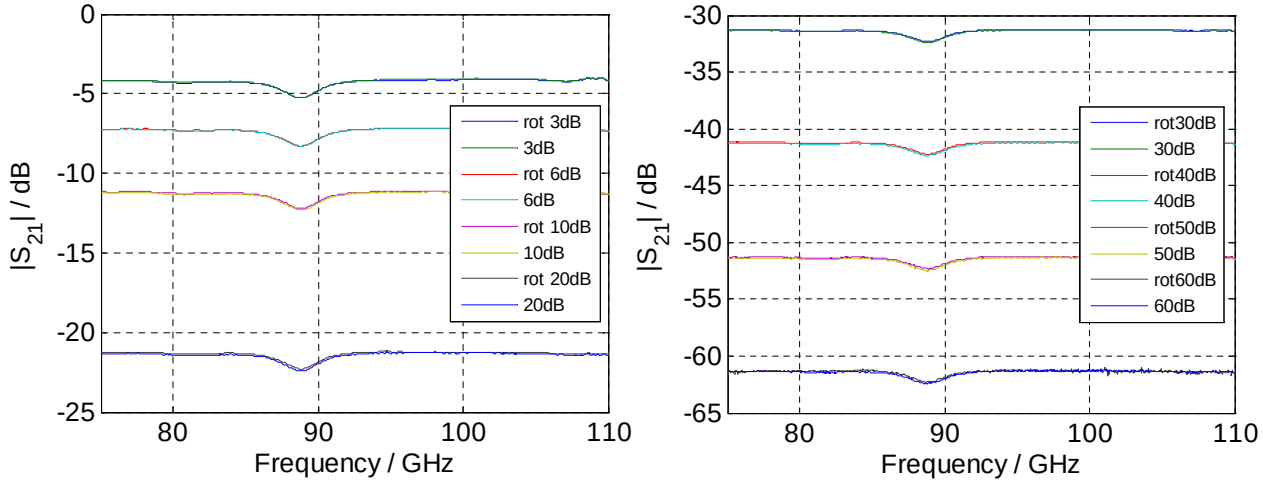

Fig. 11. Substitution of GHz attenuation provided by a precision rotary attenuator with traceably calibrated coaxial PC3.5mm attenuators at 279.28 MHz. Rot3dB indicates measurements with the PRA at a 3 dB setting, 3 dB indicates the substitution with a coaxial 3-dB-attenuator.

References

Adamson, D., Ridler, N., and Howes, J.: , Recent and future developments in millimetre and sub-millimeter wavelength standards at NPL, Proc. of the Joint 5th ESA workshop on millimetre-wave Technology and applications and 31th ESA Antenna Workshop, 463–467, Nooordwijk, The Netherlands, 2009.

Clarke, R., Pollard, R., Ridler, N., and Salter, M.: Traceability to national standards for S-parameter measurements of waveguide devices from 110 GHz to 170 GHz, Microwave Measurement Conference, June 2009, 73rd ARFTG, Boston, USA, 2009.

Hoffmann, J.: Traceable S-Parameter Measurements in Coaxial Transmission Lines up to 70 GHz, Dissertation ETH Zürich, Switzerland, 2009.

Horibe, M., Kishikawa, R., and Shida, M.: Complete Characterization of Rectangular Waveguide Measurement Standards for Vector Network Analyzer in the range of Millimeter and Submillimeter wave frequencies, Microwave Measurements Conference (ARFTG), 76th ARFTG, December 2010, Clearwater Beach, USA, 2010.

Jastrow, C., Priebe, S., Spitschan, B., Hartmann, J., Jacob, M., Kürner, T., Schrader, T., and Kleine-Ostmann, T.: Wireless digital data transmission at 300 GHz, Electron. Lett. 46, 661–663, 2010.

Judaschke, R.: Second-Order Waveguide Calibration of a One-Port Vector Network Analyzer, to be published 77th ARFTG, 2011.

Lau, Y.: Understanding the residual waveguide interface variations on millimeter wave calibration, Microwave Measurements Conference (ARFTG), 76th ARFTG, December 2010, Clearwater Beach, USA, 2010.

Lok, L. B., Singh, S., Wilson, A., and Elgaid, K.: Impact of waveguide aperture dimensions and misalignment on the calibrated performance of a network analyzer from 140 to 325 GHz, Microwave Measurement Conference, 73rd ARFTG, June 2009, Boston USA, 1–4, 2009.

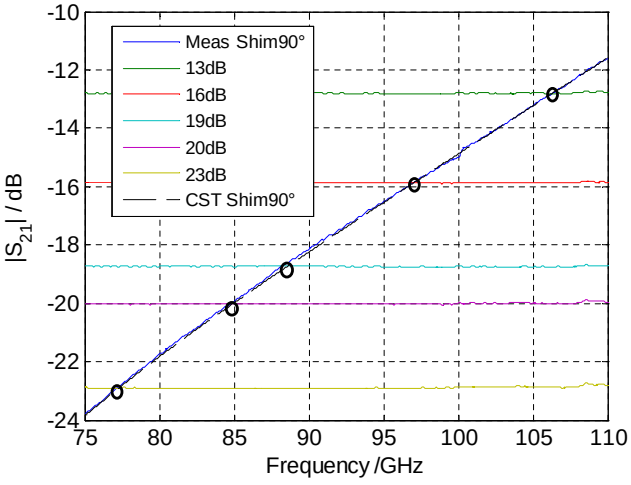

Fig. 12. Comparison of numerical simulation (CST), measurement of S_{21} of a WR10 shim rotated by 90° (HRD 90° shim), and "measurement of S_{21}" with a well-defined attenuation using coaxial attenuators inserted in the "meas in" path of the VNA covering the same dynamic range.

Priebe, S., Jastrow, C., Jacob, M., Kleine-Ostmann, T., Schrader, T., and Kürner, T.: A Measurement System for Propagation Measurements at 300 GHz, Conf. Proc. PIERS 2010, Cambridge, USA, 5–8 July, 2010

Ridler, N., Salter, M., Goy, P., Caroopen, S., Watts, J., Clarke, R., Yuenie Lau, Linton, D., Dickie, R., Huggard, P., Henry, M., Hesler, J., Barker, S., and Stanec, J.: Inter-laboratory comparison of reflection and transmission measurements in WR-06 waveguide (110 GHz to 170 GHz), Microwave Measurements Conference (ARFTG), 75th ARFTG, May 2010, Anaheim, USA, 2010a.

Ridler, N., Clarke, R., Salter, M., and Wilson, A.: Traceability to National Standards for S-parameter Measurements in Waveguide at Frequencies from 140 GHz to 220 GHz, Microwave Measurements Conference (ARFTG), 76th ARFTG, December 2010, Clearwater Beach, USA, 2010b.

Salhi, M., Kleine-Ostmann, T., and Schrader, T.: Broadband Electromagnetic Field Strength Sensors for 40-300 GHz Based on Planar Log Per Antennas and High-Speed Schottky Diodes, Conf. Proc. APMC 2010, Yokohama, Japan, 7–10 Dezember 2010.

Schrader, T., Baaske, K., Salhi, M., and Kleine-Ostmann, T.: Time-Domain Evaluation of Anechoic Environments up to 325 GHz, Conf. Proc. of 2010 Asia-Pacific Symposium on EM Compatibility, Beijing, China, 12–16 April, 2010, 778–781, doi 10.1109/APEMC.2010.5475831, 2010.

Stumper, U.: Extended Cross-Ratio Reflection Correction at Microwave Frequencies Using Waveguide Air-Lines, IEEE Transactions on Instrumentation and Measurement, 50(2), 364–367, 2001.

Williams, D. F.: Rectangular-Waveguide Vector-Network-Analyzer Calibrations With Imperfect Test Ports, Microwave Measurements Conference (ARFTG), 76th ARFTG, December 2010, Clearwater Beach, USA, 2010.